Molecular Therapy
Nucleic Acids
Original Article

Self-Amplifying Replicon RNA Delivery to Dendritic Cells by Cationic Lipids

Pavlos C. Englezou,[1] Cedric Sapet,[3] Thomas Démoulins,[1] Panagiota Milona,[1] Thomas Ebensen,[2] Kai Schulze,[2] Carlos-Alberto Guzman,[2] Florent Poulhes,[3] Olivier Zelphati,[3] Nicolas Ruggli,[1] and Kenneth C. McCullough[1]

[1]Institute of Virology and Immunology (IVI), Mittelhäusern 3147, Switzerland; [2]Department of Vaccinology and Applied Microbiology, Helmholtz Centre for Infection Research, 38124 Braunschweig, Germany; [3]OZ Biosciences, Case 922, Marseille, France

Advances in RNA technology during the past two decades have led to the construction of replication-competent RNA, termed replicons, RepRNA, or self-amplifying mRNA, with high potential for vaccine applications. Cytosolic delivery is essential for their translation and self-replication, without infectious progeny generation, providing high levels of antigen expression for inducing humoral and cellular immunity. Synthetic nanoparticle-based delivery vehicles can both protect the RNA molecules and facilitate targeting of dendritic cells—critical for immune defense development. Several cationic lipids were assessed, with RepRNA generated from classical swine fever virus encoding nucleoprotein genes of influenza A virus. The non-cytopathogenic nature of the RNA allowed targeting to dendritic cells without destroying the cells—important for prolonged antigen production and presentation. Certain lipids were more effective at delivery and at promoting translation of RepRNA than others. Selection of particular lipids provided delivery to dendritic cells that resulted in translation, demonstrating that delivery efficiency could not guarantee translation. The observed translation *in vitro* was reproduced *in vivo* by inducing immune responses against the encoded influenza virus antigens. Cationic lipid-mediated delivery shows potential for promoting RepRNA vaccine delivery to dendritic cells, particularly when combined with additional delivery elements.

INTRODUCTION

Synthetic nanoparticles can efficiently deliver antigen to targeted cells, including dendritic cells (DCs).[1] More recently, nanoparticle-mediated delivery of self-amplifying RNA replicons (RepRNA) to DCs has been forthcoming.[2–4] Indeed, synthetic chitosan-based and polyplex nanoparticulate vehicles facilitated delivery of RepRNA derived from the Pestivirus classical swine fever virus (CSFV) to DCs.[2,3] An alphavirus-derived RepRNA was also successfully delivered using lipid-nanoparticles or cationic nano-emulsion, inducing immune responses,[5–7] but there was no information on cell targeting, particularly to DCs. RepRNA, referred to as a self-amplifying mRNA when derived from positive-strand viruses, is generated from a viral genome lacking at least one structural gene; it can translate and replicate (hence "self-amplifying") without generating infectious progeny virus.[1,8–12] The RepRNA technology provides a platform for inserting new gene cassettes encoding a desired antigen of interest.[1,13–15] This has particular importance when the RNA is delivered to DCs, wherein the antigen of interest can be expressed within intracellular compartments of the cells, leading to processing and presentation to the adaptive immune system.

Although nanoparticle-mediated delivery has been reported for DNA and small RNA molecules such as siRNA and mRNA,[1] these cannot be related to RepRNA delivery because of the larger size and more complex structure of the latter.[1,15] The greater size of the RepRNA creates a distinctive molecular interaction with the delivery vehicle, the cationic components providing a higher level of complexing (nitrogen:phosphate groups; N:P ratios) with RepRNA than with smaller RNA molecules to protect it from degradation and to form small complexes that can be internalized into cells. Apart from the aforementioned analyses with chitosan-based and polyplex delivery of RepRNA,[2,3] little is known about how DCs interact with cationic nanoparticle-mediated delivery vehicles carrying relatively large self-amplifying RNA molecules.

DCs lie at the cross-roads of innate and adaptive immune responses, and they are widely acknowledged as the main inducers and regulators of adaptive immune responses.[16,17] This relates to their efficient and intricate endocytic network employed for processing antigens and their ability to migrate into key lymphoid compartments for presenting antigen to induce immune responses.[18,19] Nonetheless, although DC-oriented vaccine strategies offer high potential, DCs are inefficient at "naked" nucleic acid uptake.[1]

Delivery of replicon vaccines has primarily employed replicons derived from cytopathogenic viruses delivered as virus particles—virus replicon particles (VRPs).[1,8,9,11] These VRPs are generated by transfecting the replicons into a cell line expressing the deleted gene products to allow virus-like progeny to be formed. Nonetheless, the replication characteristics of such cytopathogenic replicons would destroy the DCs into which they are introduced, reducing the

Received 25 April 2017; accepted 29 April 2018;
https://doi.org/10.1016/j.omtn.2018.04.019.

Correspondence: Pavlos C. Englezou, The Biomedical Centre, Division of Molecular Haematology, Sölvegatan 19, 22362 Lund, Sweden.
E-mail: pavlos.c.englezou@gmail.com

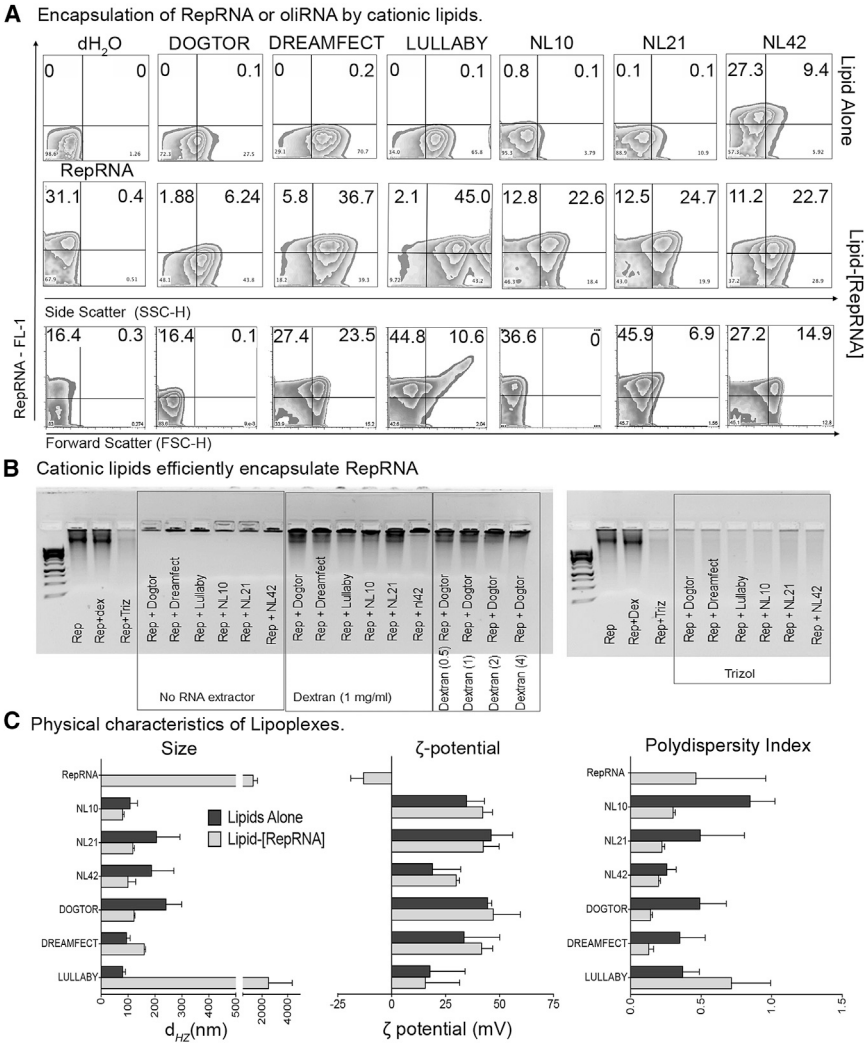

Figure 1. Encapsulation of RepRNA by Cationic Lipids

(A) Encapsulation of RepRNA by cationic lipids. FITC-labeled RepRNA (2 μg) was complexed with the various lipids of interest. Lipid-RepRNA nanoparticle complexes are detected in the side scatter (SSC-H, x axis) or forward scatter (FSC-H). The figure demonstrates the association of FITC-labeled RepRNA with the various cationic lipids of interest, providing clues for the size and "granularity" of the various lipoplexes. (B) The capacity of the various lipids of interest to complex the RepRNA was assessed with a gel retardation assay. RepRNA alone (1 μg), RepRNA in the presence of dextran sulfate, and RepRNA in the presence of TRIzol were controls for assessing lipoplexes, dextran sulfate-treated lipoplexes, or TRIzol-treated lipoplexes. RepRNA was detected using 1% (w/v) agarose gel electrophoresis at 130 V for 10–15 min. (C) Physicochemical characteristics of the lipoplexes. The physical characteristics of cationic lipids alone or carrying RepRNA were assessed in water. The various lipids or lipoplexes were characterized according to their hydrodynamic diameter (Z-average size, d_{HZ}), surface charge (ζ-potential), and polydispersity index. Measurements were conducted under dynamic light scattering at 25°C with a scattering angle of 173°.

durability of antigen presentation and promotion of adaptive immune defenses; antigen presentation by the DCs would require a secondary acquisition of antigen from cells translating the replicons. Application of non-cytopathogenic RepRNA constructs would circumvent these problems and allow direct targeting to DCs. The non-cytopathogenic RepRNA would permit a more prolonged presence of antigen, increasing the durability of antigen presentation by DCs—important for efficient promotion of adaptive immune defenses.[16,17] Non-cytopathogenic replicons employed as VRP-based vaccines have proven successful.[1,10,12]

Despite the efficiency of VRP-based delivery of RepRNA, this is encumbered by the requirement for complementing cell lines. Moreover, the approach cannot be manipulated for cell targeting, being reliant on VRP tropism (related to the virus parent of the VRPs); VRPs may also be attacked by pre-existing immunity and often display species and cell type restrictions.[1,14,15] An alternative approach to VRPs is delivery by synthetic, positively charged nanoparticles that interact with and complex the negatively charged RepRNA.[1,14,15,20–23] These vehicles are easily synthesized and can be formulated to target particular cell populations of interest, such as DCs. Accordingly, the current investigation assessed the capacity of different cationic lipids for RepRNA delivery to DCs leading to translation. These *in vitro* characteristics were related to the *in vivo* readout, measured in terms of both humoral and cell-mediated immunity, providing the first evidence of the potential of cationic lipids to facilitate delivery of large RepRNA vaccines to DCs.

RESULTS

Cationic Lipid Complexing of RepRNA

Considering the absence of information regarding cationic lipid interaction with large RNA molecules such as RepRNA, it was first important to determine whether any cationic lipid formulations could complex RepRNA molecules. Several lipids were selected from a specific library based on different hydrophobic, linker, and charge properties (Table S1).[24] To characterize how RepRNA molecules interact with different cationic lipids, RepRNA was labeled with fluorescein isothiocyanate (FITC) for visualization by flow cytometry (Figure 1A). Flow cytometry forward (FSC-H) and side scatter (SSC-H) settings were adjusted to detect the light-scattering properties of the lipids in direct comparison with diluent alone (distilled water, dH_2O), as reported for showing the association of labeled RepRNA with chitosan nanoparticles, described previously.[3] It became apparent that

different lipids displayed distinct, reproducible patterns for the interaction with RepRNA. All lipids increased their SSC-H values (Figure 1A, top compared with center, x axis) following complexing with RepRNA, but with differing degrees. Lullaby lipid-based complexes led to a strong shift in SSC-H with two separate populations; both had increased SSC-H compared with lipid alone. In contrast, DOGTOR-RepRNA complexes displayed the lowest shift in SSC-H in comparison with DOGTOR alone, suggesting that DOGTOR may compact the RepRNA molecules more efficiently to form smaller lipoplexes. Related characteristics were obtained when looking at FSC-H (Figure 1A, bottom, x axis). Again, Lullaby induced the largest shift in FSC-H, with a distinct population being evident, whereas DOGTOR (along with NL-10) appears to retain the same size as the lipid nanoparticles alone (data not shown).

When the association of the labeled RepRNA (Figure 1A, y axis) was interrogated, this elaborated the above observations. DOGTOR-based complexes gave the lowest shift for associated RNA (Figure 1A, y axis and top right quadrants). However, the RepRNA signal (as shown with dH_2O) was strongly reduced in the presence of DOGTOR, suggestive of possible quenching, which could have arisen because of the aforementioned proposed strong compaction by the lipid. The other lipid-RepRNA complexes all showed a signal relating to the RepRNA signal in dH_2O, although the results with NL-42 were unclear because of the lipid alone presenting a signal in the FL-1 channel—used to detect the RepRNA-FITC—probably related to autofluorescence.

Following interaction with 1 μg RepRNA, the gel retardation assay (Figure 1B) demonstrated that all cationic lipids under assessment successfully complexed the large RNA molecules, observable within 20 min (Figure 1B, No RNA Extractor). The complexed RepRNA was partially released following treatment with 1 mg/mL dextran sulfate (Figure 1B, dextran [1 mg/mL]), relating to previous results employing dextran sulfate to release RNA from lipoplexes.[25] However, this gel-based assay cannot be employed to quantify the amount of RNA present. Consequently, the gel retardation assay was employed to ascertain whether the RepRNA would remain at the top of the gel, indicative of complexing with the lipids and, therefore, confirming the results obtained by flow cytometry (Figure 1A).

In addition, the gel retardation assay was performed under non-sterile, non-RNase-free conditions to assess the presence of RepRNA smearing, which would be indicative of RNA degradation. This was sought because of the observations with lipid complexing of DNA, which showed that DNA was protected from degradation, even after 24 hr incubation in 50% fetal calf serum (FCS) at 37°C (data not shown). When EDTA was added to stop the nuclease action and DNA was released from the complexes with dextran sulfate, no degradation of the DNA was observed, contrasting with the non-complexed DNA that showed degradation after only 45 min in 50% FCS (data not shown). The results with lipid complexing of RepRNA molecules indicated that the RepRNA was also protected from degradation (no smearing; Figure 1B, no RNA extractor) unless the complexing was destabilized by dextran sulfate treatment (Figure 1B, dextran [1 mg/mL]); see also Figure 4a). Nonetheless, it was noted that the attempted destabilization of lipoplexes by dextran sulfate did not apparently promote release of all of the RNA from the complexes. We therefore assessed RNA dissociation from the lipids using an increasing concentration of dextran sulfate with DOGTOR-associated lipoplexes (Figure 1B, dextran (0.5), dextran (1), dextran (2), dextran (4)). The results revealed that the activity of dextran sulfate was most efficient at dissociating the RNA from the lipoplexes at the lower concentrations (0.5 and 1 mg/mL). Treatment with dextran sulfate also suggested that dissociation of the RepRNA from DOGTOR and NL21 was potentially more effective, as evidenced by the thicker bands of RepRNA observed (Figure 1B, dextran (1 mg/mL)).

Considering that dextran sulfate treatment may have proven to be inefficient at releasing all RepRNA molecules from the lipoplexes, we also employed treatment with TRIzol solution. We routinely employ this for extraction of RNA, and it is likely more effective at dissociating RepRNA from the lipoplexes. Although TRIzol treatment initially appears to have no detrimental effect on RepRNA, the RNA no longer has the stability observed with material before such treatment and rapidly degrades. This sensitivity of RepRNA for TRIzol treatment can be seen in Figure 1B, Rep+Triz compared with Rep and Rep+Dex. Consequently, TRIzol treatment could only be employed to assess the RepRNA by gel analysis and not by functionality. Despite this sensitivity of RepRNA to TRIzol treatment (Figure 1B, Rep+Triz), it was clear that TRIzol treatment of the lipoplexes was successful at releasing the RepRNA (Figure 1B, TRIzol). This was observed by the absence of a clear RNA band near the well area of the gel, contrasting with the distinctive band observed with untreated lipoplexes and dextran sulfate-treated material (Figure 1B, no RNA extractor and dextran (1 mg/mL)). Although TRIzol resulted in degradation of the RepRNA, as observed with RepRNA alone treated with TRIzol (Figure 1B, Rep+Triz), the release of RNA was observed by faint smears on the gel (confirmed by an overexposed image of the gel; data not shown).

Although treatment with dextran sulfate and TRIzol solution confirmed that the RepRNA was associated with the lipids, neither treatment could permit any interpretation of manipulation of the lipoplexes by the cells either *in vitro* or *in vivo*. It is impossible to mimic the endocytic processes within the cell that would lead to release of the RNA from the lipoplexes. Albeit one may infer the relative degree of dissociation, the levels of translation obtained within cells and following *in vivo* administration, are due to the much more complex manner by which cells will handle the lipoplexes and how this can promote cytosolic translocation of the RepRNA into intracellular translation sites.

Physical Properties of Cationic Lipid Complexes with RepRNA

Considering the above observations, it was important to assess the size (hydrodynamic diameter, d_{HZ}), ζ-potential, and polydispersity index (PDI) of the lipoplexes (Figure 1C). Most of the cationic lipid

formulations showed a small decrease in d_{HZ} following association with RepRNA (Figure 1C, Size), reflecting efficient compaction and formation of small lipoplexes. Dreamfect-based lipoplexes had a small increase, whereas the increase in d_{HZ} for the Lullaby-based complexes was more notable. The value for the latter related more to the d_{HZ} obtained with the RepRNA alone, which may reflect poor or no compaction of the RepRNA by Lullaby, despite clear interaction (Figures 1A and 1B). These results are in good agreement with those from the flow cytometry (Figure 1B), again suggesting that different lipids may be distinctive in how they complex and potentially compact RepRNA molecules; the majority appear to form lipoplexes quite efficiently with the RNA. The apparently large Lullaby-based complexes with RepRNA molecules, apparently in the micron range, also relate to the results observed with the flow cytometry analysis.

In contrast to the d_{HZ}, the ζ-potential of the cationic lipids remained largely unaffected by lipoplex formation. Although quite distinctive for each cationic lipid, relating to their structures and charge, all lipoplexes remained, as expected, within the positive range because of amine groups present in the polar head of the lipids being used in excess compared with phosphate groups of the RNA, demonstrating the dominance of the lipid charge at their surfaces. With the lipid PDI, this was similar to the d_{HZ} observations in being generally reduced following lipoplexing with the RepRNA molecules because of the higher heterogeneity of lipoplexes. Only the Lullaby-based lipoplexes showed a PDI increase, again in the range observed with RepRNA alone. Among the other lipids, the largest PDI reduction was observed with NL-10 lipoplexes, which highlighted a great heterogeneity of lipoplexes sizes. These results suggest that all cationic lipids, with the exception of Lullaby, were complexing and likely compacting the RepRNA molecules. Certainly, with Lullaby, the less-charged formulations also formed lipoplexes with the RepRNA, as observed by gel retardation, flow cytometry, and increased d_{HZ} and polydispersity, but the complexes may have less compaction compared with the other lipid-based lipoplexes.

Lipid-Mediated Delivery and Translation of RepRNA Molecules to Porcine DCs and Monocytes *In Vitro*

Although it was interesting to observe that the different cationic lipids were somewhat distinctive in complexing the RepRNA, it was important to see how this related to the intracellular delivery of RepRNA to DCs. Because of previous reports of efficient lipoplex delivery of small nucleic acid molecules, such as DNA and siRNA,[26] complexing of FITC-RepRNA and FITC-oligoRNA were compared regarding delivery to porcine blood DCs and monocytes. Delivery of oligoRNA or RepRNA in the absence of a delivery vehicle was negligible, whereas their complexing to lipid formulations markedly enhanced the delivery to both DCs and monocytes (Figures 2A and 2C). $CD172a^{hi}$ cells are primarily monocytes with classical DC (cDC)1 cells, whereas $CD172^{low}$ cells primarily contain cDC2 cells with no monocytes[27] (representative histograms of a single experiment are shown in Figure 2C, whereas Figure 2A shows the mean ± SD from different replicates). Delivery of lipid-oligoRNA complexes was always significantly higher in comparison with RepRNA (Figure 2C) in both DCs and monocytes. NL-10, NL-21, and NL-42 were seen to be the most efficient carriers for delivery of RepRNA to both $CD172^{hi}$ and $CD172^{low}$ cells (Figure 2A). The other lipids tended to favor more selective delivery, particularly DOGTOR- and Lullaby-based lipoplexes were targeting the $CD172^{hi}$ cells more.

The lipid-dependent pattern for lipoplex delivery of RepRNA was clearly distinctive from that with oligoRNA, demonstrating that it is impossible to infer from studies with oligoRNA (and also from small mRNA molecules; data not shown) how lipids could be applied with larger RepRNA. The cationic lipids could be classified in two "groups" with respect to the characteristics of RepRNA molecule delivery. NL-10 (∼180 a.u.), NL-21 (∼150 a.u.), and NL-42 (∼100 a.u.) showed a greater relative efficiency of lipoplex-based RepRNA delivery to both $CD172^{hi}$ and $CD172^{low}$ cells (Figures 2A and 2C, bottom). Dreamfect, DOGTOR, and Lullaby displayed a markedly lower relative efficiency of lipoplex-based delivery of RepRNA to both $CD172a^{+}$ cell populations (Figures 2A and 2C). Moreover, Dreamfect, DOGTOR, and Lullaby-based delivery tended to favor $CD172a^{hi}$ cell interaction. The observed differences in these two groups of lipids regarding lipoplex-based RepRNA delivery were statistically significant, as exemplified when comparing NL-10-, Dreamfect-, and DOGTOR-assisted transfections (Figures 2A and 2C). To address whether the increased efficiency of RepRNA delivery was associated with lipid-mediated induced cytotoxicity, we investigated both the viability of cells treated with RepRNA-unrelated lipids and interrogated the percentage of viable cells within the $RepRNA^{+}$ cell compartment for each lipid of interest (Figure S2). The results suggest that the enhanced efficiency of delivery observed with NL-10, NL-21, and NL-42 was not a result of passive RepRNA entry because of cell death.

To determine whether the results were influenced by the effect of the lipoplexes on the cells, the cell membrane integrity of both $CD172^{hi}$ and $CD172^{low}$ cells was assessed 2 hr after lipofection using 7-aminoactinomycin (7-AAD) staining (Figure 2B). Cells treated with "naked" RepRNA or lipids alone (data not shown) gave a background signal, obtained with untreated cells, ranging from 5% to 30% of labeled cells (Figure 2B, RepRNA); this may be reflecting the "background" characteristics of the cell membranes and/or the characteristics of these primary cells in culture. Compared with these controls, the lipoplexes generally showed an insignificant reduction in the viability of both $CD172^{hi}$ and $CD172^{low}$ cells. The exception was NL10 (30%–35% over the controls), although this demonstrated that the effect of lipoplexes on cell integrity remained minimal. Increasing the amount of lipids applied to the cells did not alter this observation (examples of the lipids are shown in Figure S1). Nonetheless, such observations could have an effect on induction of adaptive immunity in general and the role of the cDC2 subset in particular. These results also have to be put in perspective because it is known that, during the first hours following initiation of transfection, cell membrane integrity can be altered by the transfection mechanisms involving cationic lipids or polymers. Nonetheless, one

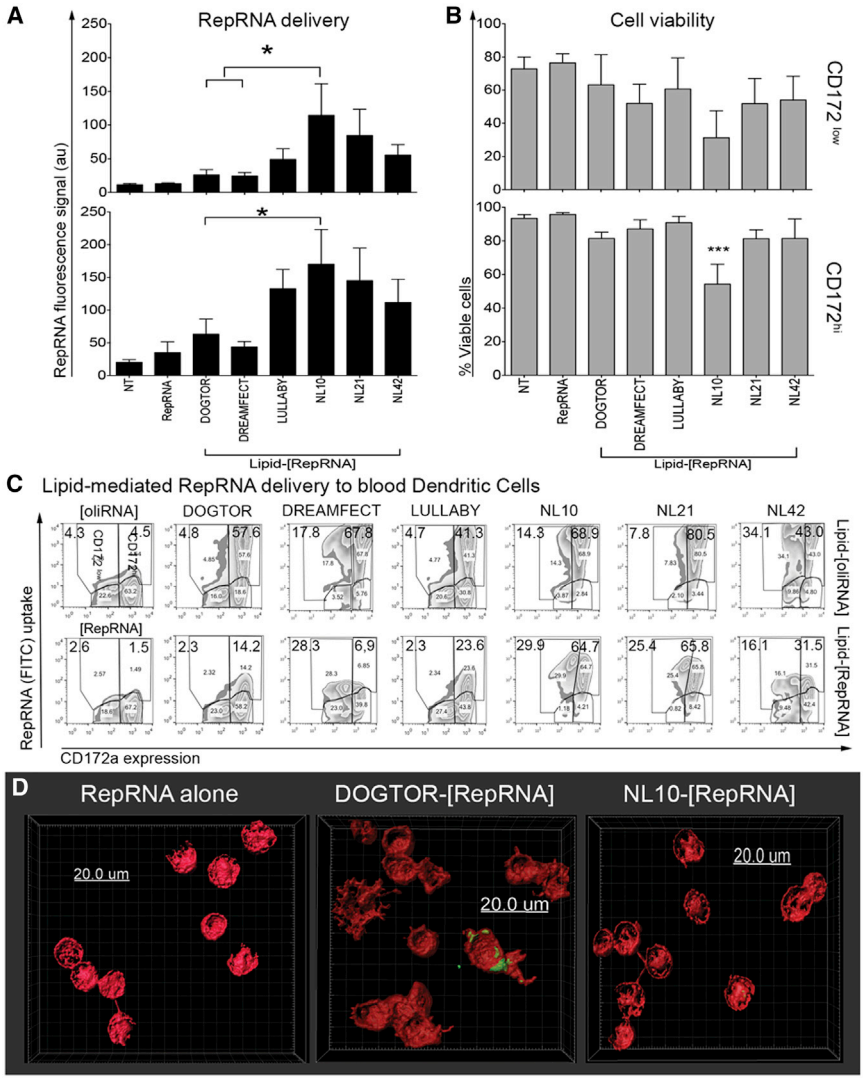

Figure 2. Lipid-Based Delivery or Binding of RepRNA to Porcine DCs and Monocytes *In Vitro*

FITC-labeled RepRNA (2 μg/10^6 cells) or FITC-labeled oliRNA was complexed with the different lipids of interest and applied to CD172a-selected PBMCs for 2 hr. (A) Percentage of cells positive for RepRNA (oliRNA data not shown). The x axis depicts the different lipids of interest, whereas the y axis indicates the intensity of RepRNA delivery. (B) Cell viability of DCs and monocytes 2 hr after treatment with the lipoplexes, as assessed with 7-aminoactinomycin-D staining. (C) Representative histograms with respect to RepRNA delivery. Data are displayed as mean ± SEM (n = 3 independent experiments), and statistical significance of differences between groups was assessed by one-way ANOVA and Dunnett's multiple comparisons *post hoc* test (*$p < 0.05$). (D) Intracellular delivery of RepRNA to porcine DCs and monocytes. Cells were pulsed with FITC-labeled RepRNA for 2 hr before samples were labeled for CD172a (red). Analysis was performed with the IMARIS 7.7 software to generate high-resolution 3D stacks and assess RepRNA delivery. The scale bars indicate 20 μM.

particular lipoplex composed of NL-10, the most charged lipid, seems to have a negative effect on DCs, as shown in Figure 2C, although this may simply reflect the larger number of cells receiving RepRNA, as shown in Figures 2A and 2C.

To confirm that the above results were reflecting RepRNA internalization rather than binding to the cell surface or recycling, lipoplex delivery was assessed with confocal microscopy and 3D imaging. Uptake at 2 hr after lipofection (Figure 2D clearly shows two of the lipids representative of the aforementioned two groups). This was more apparent with lipoplexes from the groups represented in Figure 2D by DOGTOR-RepRNA than with the other lipids of interest (represented by the NL-10 image in Figure 2D).

Delivery of RepRNA to DCs is only the starting point; the ultimate requirement is delivery leading to RepRNA translation. Intracellular delivery of RepRNA will not necessarily result in RNA translation. For this, the lipoplexes need to be internalized in a manner promoting access to the cytosolic compartments of the target cells but also have to allow the decompaction of the RepRNA necessary for facilitating the intrinsic ability of RepRNA to be translated. The results regarding the ability of the lipids to interact, complex, and protect the RepRNA shown in Figure 1 raised questions about the capacity of intracellular decompaction/release of the RepRNA in terms of RepRNA integrity and accessibility to the ribosomal translational machinery.

RepRNA translation following lipofection was assessed using expression of the NS3 protein, one of the RepRNA-encoded antigens and an important component of the replication complex (Figures 3A and 3B). Freshly isolated CD172a-enriched peripheral blood mononuclear cells (PBMCs) were pulsed with either naked RepRNA or RepRNA associated with the various cationic carriers. When observed beyond the short time points employed for delivery assessment, a common finding is down-regulation of CD172 expression *in vitro*, including the controls, rendering distinction of $CD172^{low}$ and $CD172^{hi}$ subpopulations difficult (Figure 3A). In accordance with previously published data, naked RepRNA delivery to DCs and monocytes does not result in translation (Figure 3A). Evidence of NS3 expression and, therefore, RepRNA translation (at the 72-hr time point example shown in Figure 3A) was found with lipoplexes formed with three of the lipids: Dreamfect (21.6%), Lullaby (11.3%), and NL-42 (11.3%). The percentage of cells positive for antigen translation varied between VRPs and lipofections of PBMCs isolated from different cell preparations derived from different animals (Figures 3A and 3B). Indeed, as illustrated in

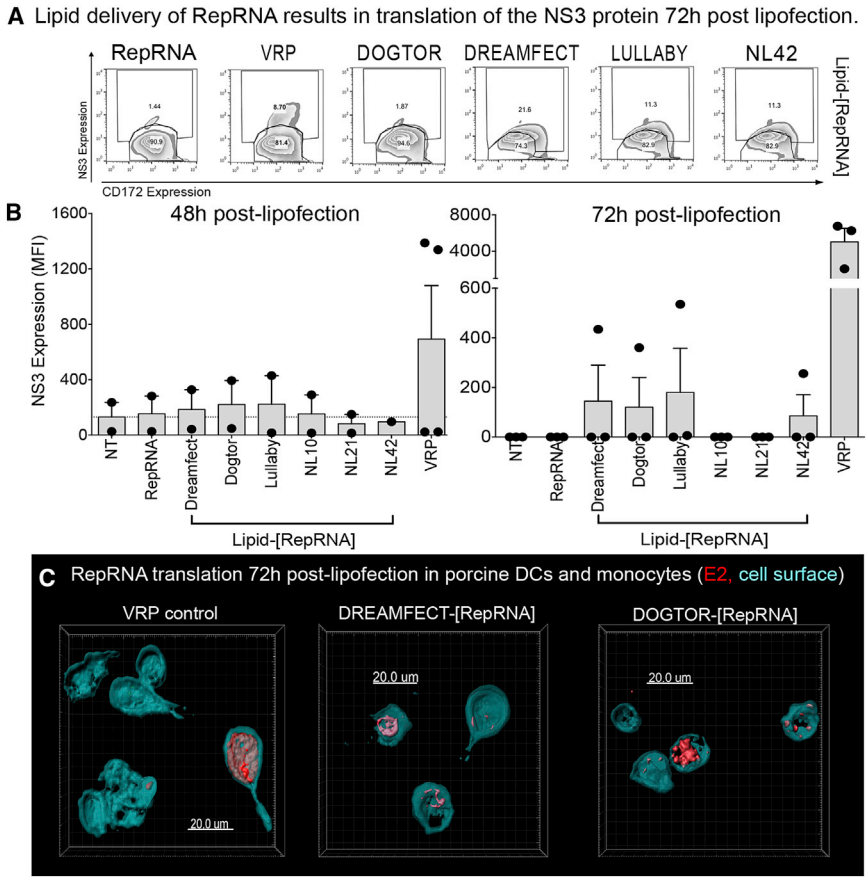

Figure 3. Cationic Lipids Facilitate RepRNA Delivery for Translation in Porcine DCs and Monocytes *In Vitro*

RepRNA (2 μg/10^6 cells) was complexed with the different lipids of interest and applied to freshly isolated CD172-enriched PBMCs for 2 hr. RepRNA translation (NS3 expression) was assessed with flow cytometry 48 and 72 hr post-transfection, and VRPs were employed as a positive control. (A and B) Data are shown as (A) representative histograms and with respect to (B) percentage of positives for NS3 translation and are displayed as mean ± SEM (n = 3 independent experiments). Statistical significance of differences between groups was assessed by one-way ANOVA and Dunnett's multiple comparisons *post hoc* test (*$p < 0.05$). (C) RepRNA translation was also assessed using confocal microscopy 72 hr post-lipofection. Cells were pulsed with 2 μg/10^6 cells of RepRNA complexed with the various lipids of interest for 2 hr. The lipoplexes were removed, and the cells were fixed, permeabilized, and labeled for E2 protein (red) and a cell surface lipophilic dye (WGA633, blue) 72 hr post-lipofection. Analysis was performed using the IMARIS 7.7 software to generate high-resolution 3D stacks to assess RepRNA translation. The scale bars indicate 20 μM, and data are shown only for positive results.

Figures 3A and 3B, quantitative measurement by flow cytometry showed the VRPs to be more efficient than the lipoplexes for delivery leading to translation, most clearly at 72 hr. Consequently, translation of the delivered RepRNA was also assessed in terms of E2 expression, one of the structural proteins encoded by RepRNA and more readily detectable. With these assays, E2 translation was only detected following lipofection of RepRNA with the Dreamfect and DOGTOR lipids (Figure 3C). The E2 produced as free antigen would assemble within the virus particle, had the analyses been performed with virus, but both the free antigen and the virus particles are detectable with the antibody employed. In contrast, NS3 associates with other non-structural proteins to form the replication complex for both the virus genome and the RepRNA, anchoring into the endoplasmic reticulum (ER) by the p7 protein. Therefore, it is feasible that detection of NS3 may only be transient, but when it is within the replication complex, it may become unavailable to detection by the anti-NS3 antibody employed. Indeed, detection of NS3 is less efficient than detection of E2 during CSFV infection.

Microscopy analyses offered the opportunity to investigate RepRNA translation at the single-cell rather than population level. Although it is not possible to compare microscopy directly with flow cytometry analysis, it offered important insights into the analyses, particularly when combined with assessment of the flow cytometry. Importantly, DOGTOR was the most consistent of the lipids to promote delivery of the RepRNA leading to translation with a given ratio of formulation and over time (in experiments with cells from different donors). Nonetheless, the distribution within positive cells was somewhat distinctive from that observed with VRP delivery.

Influence of the RepRNA Load during Lipoplex Formulation on RepRNA Interaction with Lipoplexes and Their Physicochemical Properties

The above data show the relative ability of lipids to complex, protect, deliver, and ultimately facilitate translation of the RepRNA in DCs. Such observations indicated that an appropriately selected lipid carrier may be applicable for transfection of DCs for translation *in vivo*. It was therefore important to ascertain whether the transfection efficiency of the lipoplexes could be enhanced by modifying the RepRNA cargo. Thus, DOGTOR and NL-10 were selected as representative of these two groups to investigate whether increasing loads of RepRNA (2–8 μg in the lipid-RNA mix) or lipids (Figure S1) when forming the lipoplexes would influence the transfection efficiency of DCs *in vitro*. When the lipoplexes were controlled with our established gel retardation assay (Figure 4A), both DOGTOR and NL-10 complexed increasing loads of RepRNA with similar efficiency, and the complexes could be partially dissociated with dextran sulfate (1 mg/mL).

In relation to the size of these lipoplexes, there was no significant alteration in the lipoplexes with increasing concentrations of

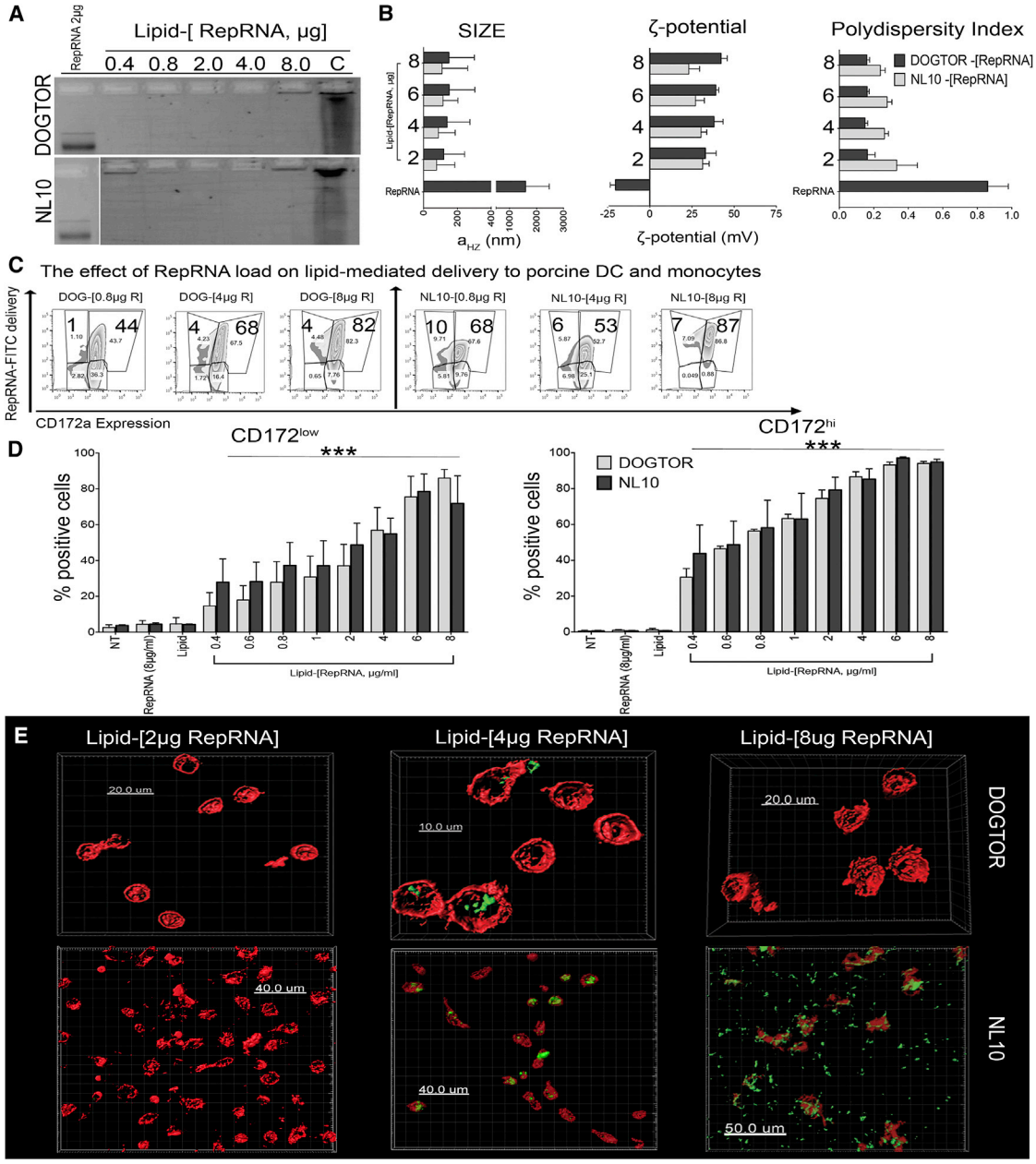

Figure 4. The Effect of RepRNA Load on the Efficiency of Delivery in DCs and Monocytes

(A–E) The capacity of the various lipids of interest to complex increasing loads of RepRNA (0.4–8 µg/mL) was assessed with a gel retardation assay. RepRNA alone, lipoplexes, or lipoplexes treated with dextran sulfate were assessed with 1% agarose gel electrophoresis at 100 V for 30 min (A). The physical characteristics of cationic lipids alone or carrying increasing loads of RepRNA (2–8 µg/10^6 cells) were assessed in water. The various lipids or lipoplexes were characterized according to their hydrodynamic diameter (d_{HZ}), ζ-potential, and polydispersity index. Measurements were conducted under dynamic light scattering at 25°C with a scattering angle of 173° (B). A range of increasing loads of FITC-labeled RepRNA (0.4–8 µg/10^6 cells) was complexed with either DOGTOR or NL-10 and used to lipofect freshly isolated CD172-enriched PBMCs for 2 hr. Cells were analyzed for RepRNA delivery using flow cytometry. Data are shown as representative histograms for RepRNA delivery, where the x axis depicts CD172a expression and the y axis the intensity of RepRNA-FITC delivery (C). Data are also displayed as percentage of positives (mean ± SEM, n = 3 independent experiments) for RepRNA in $CD172^{low}$ and $CD172^{hi}$ (D). Statistical significance of differences between groups was considered by one-way ANOVA and Tukey's multiple comparisons *post hoc* test (***$p < 0.001$). RepRNA delivery was also assessed using confocal microscopy 2 hr post-lipofection. Cells were pulsed with 2 µg/10^6 cells of FITC-RepRNA (green) complexed with the various lipids of interest. The lipoplexes were removed, and the cells were labeled against CD172a (red). Analysis was performed using the IMARIS 7.7 software to generate high-resolution 3D stacks to assess RepRNA translation. The scale bars indicate a relative distance in micrometers (E).

RepRNA molecules in the formulation mixture (Figure 4B). The results suggest that NL-10 may compact RepRNA molecules more efficiently, although the difference compared with the other lipoplexes was minor. With regards to the charge, increasing the anionic RepRNA load in the formulation mixture did not significantly affect the net positive charge of the lipoplexes. Nonetheless, the increasing RepRNA load when preparing the DOGTOR-RepRNA complexes appeared to create a minor increase in ζ-potential (~5 mV), whereas the opposite effect was observed with NL-10-based lipoplexes. As for the PDI, with the DOGTOR lipoplexes it remained constant (~0.2) with an increasing RepRNA load applied in the mixture, whereas a slightly negative correlation was observed with NL-10 lipoplexes (0.28–0.35), suggesting perhaps that DOGTOR complexes are more stable structures (Figure 4B).

Influence of the RepRNA Load during Lipoplex Formulation on Lipoplex Delivery to DCs

The influence of associating increasing loads of RepRNA during formation of the lipoplexes was also assessed for delivery to DCs (Figures 4C and 4D). A positive dose-dependent correlation was observed with both lipids; an increasing amount of FITC-labeled RepRNA molecules associated with both $CD172^{hi}$ and $CD172^{low}$ cells. The reduced efficiency of "delivery" with the lower cargo loading of RepRNA is more obvious with the $CD172^{low}$ population of cells. Similar observations were obtained with increased loading of lipids (Figure S1).

To examine whether the interaction of the lipoplexes shown in Figures 4C and 4D reflected solely binding or true uptake by the DCs, confocal microscopy and 3D imaging were employed (Figure 4E). Optimum delivery, following 2 hr treatment of DCs with the lipoplexes, was observed with the 4 μg/mL RepRNA load, and selecting the appropriate ratio of lipid RepRNA provided for maximum delivery efficiency, as shown in Figure S1. Higher concentrations did not provide detectable delivery with DOGTOR in certain experiments (an example of this is shown in Figure 4E), whereas higher RepRNA loads with NL-10 led to an image typical of aggregation (an example of this is also shown in Figure 4E; particularly evident are the clear extracellular aggregates). Such apparent aggregation was not identified with the physicochemical assessment (Figure 4B), suggesting that the phenomenon only occurred upon interaction with the cells in the cell culture medium during the first 2 hr of incubation.

The observations that higher loads of RepRNA were less favorable for lipoplex formation may also be related to an alteration in the viability of the cells. Microscopy observations showed a relative decrease in cell viability with the highest concentration of RepRNA molecules, in contrast with the highest dose of lipids (Figure S1A). Importantly, this highest concentration of RepRNA is out of the range recommended for *in vitro* delivery and, therefore, beyond the classical threshold observed for all positively charged transfection formulations (data not shown). Nonetheless, the concentration of the RepRNA load when forming immune complexes has to be chosen carefully to ensure adequate complexing by the lipids without a detrimental influence on the cells.

Influence of the RepRNA Load during Lipoplex Formulation on RepRNA Translation following Delivery to DCs

Following delivery of the lipoplexes shown in Figure 4 to DCs, it was essential to determine whether this led to translation of the RepRNA. Initially, we attempted to assess the translation of the RepRNA with flow cytometry; however, this has proven unfruitful (Figure S3). We have thus assessed RepRNA translation by E2 expression using confocal microscopy and 3D imagery (Figure 5). It was clearly evident that increasing the load of RepRNA had an effect on the transfection efficiency for both DOGTOR and NL-10-lipoplexes. An increase from 4 to 8 μg/mL of RepRNA cargo saw an increase in the number of cells positive for E2 expression for both lipoplexes. This apparent increase in transfection efficiency was more evident in cells treated with NL-10 lipoplexes. A further 2-fold increase in RepRNA load (16 μg/mL) did not result in a similar enhancement in RepRNA translation with DOGTOR-RepRNA-transfected cells, probably related to the observed reduction of cell viability with higher doses. However, it is clear that there is a discrepancy between delivery and translation with lipoplex formulations generated using both lipids. Although increasing the RepRNA load can increase both delivery and translation efficiencies, this was not in parallel. When translation was obtained, this occurred in cells treated with lipoplex formulations having the highest RepRNA load.

RepRNA Translation *In Vivo* following Lipoplex Delivery

To ascertain whether the above results could be applicable to vaccine delivery, the capacity of the lipids to deliver RepRNA encoding influenza virus nucleoprotein (NP) for translation *in vivo* was assessed. DOGTOR was selected for these investigations because of its consistency for delivery of RepRNA leading to detectable translation *in vitro*, along with good biocompatibility. BALB/c mice received 3 vaccinations of DOGTOR-RepRNA lipoplexes, as described in the Materials and Methods, supplemented with MALP-2 adjuvant.[28–30]

Lipid or RepRNA alone failed to induce any specific immune responses (Figure 6A), whereas DOGTOR-RepRNA lipoplexes induced significant titers of anti-NP antibodies in the sera of vaccinated animals. Related to this, B cell ($CD19^+CD45R^+CD24^+CD21^{lo}IgM^+IgD^{low}$) and memory $CD4^+$ or $CD8^+$ T cell lymphocyte frequencies ($CD3^+CD44^{hi}CD62L^{hi}CD25^+CD69^+$) were also increased in animals receiving the lipoplexes (Figures 6 and 6C). For this reason, a comparison was made between cells re-stimulated with recombinant NP protein and untreated cells from the same animal. Animals vaccinated with the RepRNA alone showed a mean stimulation index ≤ 2. The clearest evidence for specific B lymphocyte responses (stimulation index ~4) was detected in re-stimulated, undifferentiated splenocytes from animals that received the DOGTOR-RepRNA lipoplexes (Figure 6B). Specific responses were also detected with re-stimulated $CD4^+$ and $CD8^+$ memory T lymphocytes from the lymph nodes of these animals (stimulation index ~3) but not with cells from the spleen (Figure 6C).

The *in vivo* observations were consolidated by the cytokine profiles observed in the serum (Figure 7). DOGTOR-RepRNA lipoplex

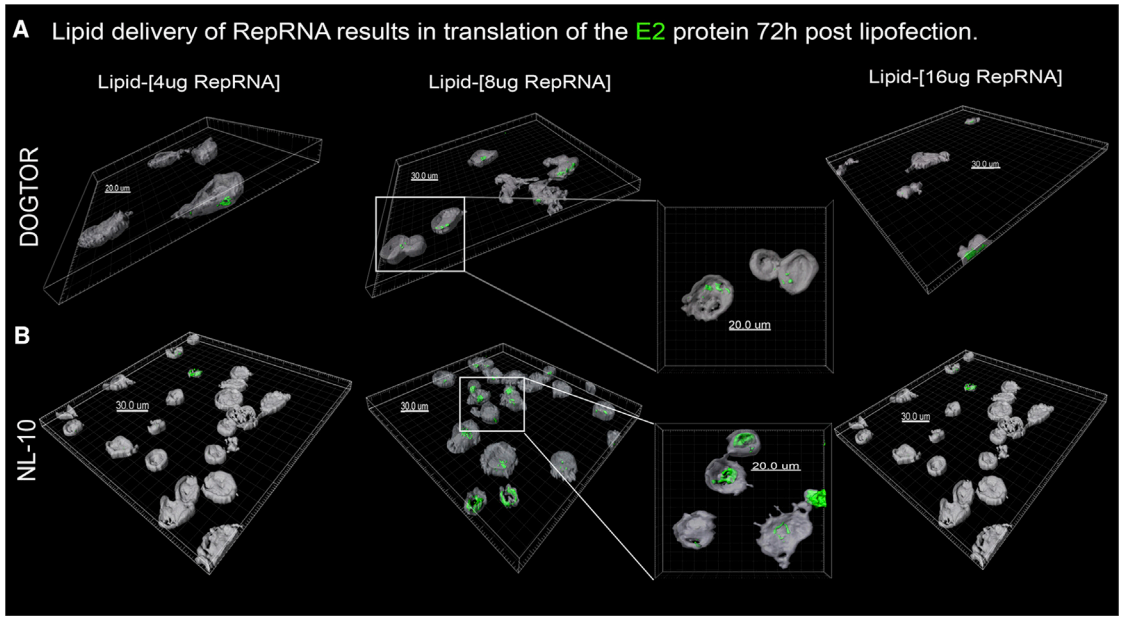

Figure 5. The Effect of RepRNA Load on the Efficiency of Translation in DCs and Monocytes

A range of increasing loads of RepRNA (0.4–16 μg/10^6 cells) was complexed with either DOGTOR (A) or NL-10 (B) and applied to freshly isolated CD172-enriched PBMCs for 2 hr. RepRNA translation was assessed by E2 (green) expression 72 hr later while the cell surface was stained with WGA-633 (gray). Threshold subtraction and gamma-correction for all images acquired were set as in the control non-treated group (data not shown). All scale bars indicate a relative distance in micrometers.

vaccination induced significant levels of interferon γ (IFN-γ) (~5,000 pg/mL; Figure 7A) in comparison with vaccination with RepRNA alone or DOGTOR alone (~2,000 pg/mL). The lipoplexes also influenced both interleukin-4 (IL-4) (5-fold increase) and IL-13 (6-fold increase) induction, again markedly higher than the levels detected in sera from RepRNA alone- or DOGTOR alone-vaccinated animals (Figure 7B). A similar pattern of enhancement was observed with IL-6 release, contrasting with tumor necrosis factor alpha (TNF-α) levels, which were not influenced by employment of lipoplexes, rather than free RepRNA (Figure 7C). IL-17 and IL-22 levels were also higher in sera from animals receiving the lipoplexes compared with animals receiving RepRNA alone or DOGTOR alone (Figure 7C).

DOGTOR-RepRNA Lipoplexes Rather Than Emulsions Induce Specific T Lymphocyte Responses

To consolidate the cellular responses against influenza virus NP antigen identified in Figures 6 and 7, an adoptive transfer model for characterizing immune responses was employed. This model provides a platform to determine whether the translation observed *in vitro* could be reflected in terms of inducing an *in vivo* immune response. The model antigen for this adoptive transfer is derived from the ovalbumin (OVA) protein, the sequence of which was cloned into our RepRNA construct as described in Materials and Methods. This cloned RNA sequence contained the specific epitope for stimulating antigen-specific $CD8^+$ and $CD4^+$ T lymphocyte clones present in OVA-transgenic major histocompatibility complex (MHC) class I (OT-I) and MHC class II (OT-II) mice, respectively.

In this experimental design, undifferentiated splenocytes and lymph node cells from OT-I or OT-II mice were pulsed with RepRNA alone or DOGTOR-RepRNA lipoplexes. The pulsed splenocytes were subsequently injected into OT-I or OT-II mice, and specific T lymphocyte responses were assessed both in the lymph nodes (Figures 8A and 8B) and the spleen (Figures 8C and 8D). In the lymph nodes, no significant responses were detected for $CD4^+$ T lymphocytes, and a positive effect was measured for $CD8^+$ T lymphocytes (Figure 8A). When assessing the splenocytes, it was the mice injected with cells pulsed using lipoplexes that provided higher stimulation indices (Figures 8C and 8D). The lipoplexes induced the most statistically significant levels of proliferation when the $CD8^+$ T lymphocyte responses were assessed (Figure 8D). Taken together with the previous *in vivo* experiment, it is clear that DOGTOR-RepRNA lipoplexes can promote cellular immune responses in an adoptive transfer model or after subcutaneous injection.

DISCUSSION

With infectious diseases posing a continuous threat to human health, vaccination has proven to be a major asset, especially for the prevention of viral infections. However, designing an effective vaccination strategy against continuously evolving pathogenic viruses, such as the highly pathogenic avian influenza, is becoming increasingly challenging. Classical vaccination strategies using inactivated viruses are encountering increasing problems, particularly because of newly emerging viruses displaying high infectivity and mortality and the high rate of antigenic shift or even drift observed with influenza viruses. Thus, there is a growing interest in the development of new

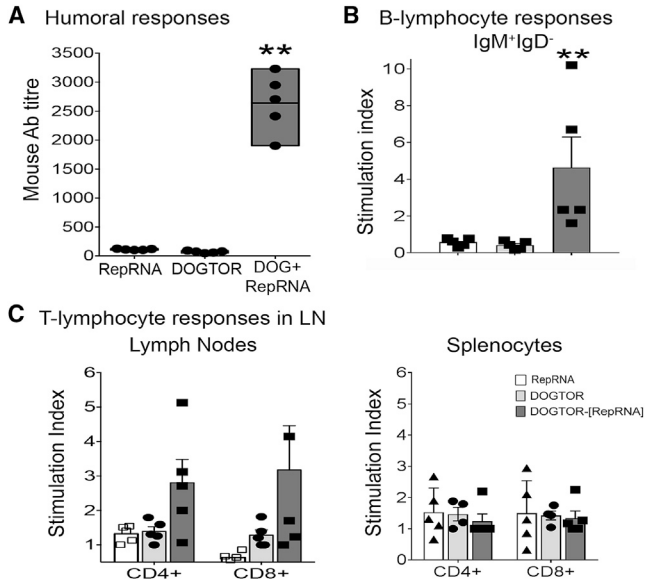

Figure 6. Cationic Lipids Deliver RepRNA for Translation *In Vivo*

Experimental animals (n = 5) received a subcutaneous vaccination cocktail on days 0, 28, and 56 comprised of 0.4 μg of NP-RepRNA complexed with DOGTOR. The vaccination cocktail was adjuvanted with PEGylated Malp-2. RepRNA alone, DOGTOR alone, PBS (data not shown), and VRPs (data not shown) were used as control groups. (A–C) Serum samples (collected on day 63 post-vaccination) were assessed for anti-NP antibody responses, whereas spleens and lymph nodes were processed, cultured, and assessed for antigen-specific proliferation responses in memory B lymphocytes (B) (splenocytes only) and central memory T lymphocytes (C) 7 days after re-stimulation with recombinant NP protein. (A) Data are shown as mean (n = 5 animals) boxplots, with each dot representing anti-NP antibody responses in a single animal, quantified by ELISA, where the x axis indicates days after vaccination and the y axis the value of anti-NP antibody titer. (B) Multiple combination labeling ($CD45^+CD19^+CD24^{2+}$ $CD21^+$ IgM^+IgD^{low}) was employed to identify memory B lymphocyte subsets. Cell proliferation was quantified as a reduction of CFSE signal as percent of cells gated as $CFSE^{low}$, indicating cell division. Stimulation indices were determined relative to the percent of cells gated as $CFSE^{low}$ obtained in the non-stimulated control. Data are shown as mean stimulation indices, with each dot representing the stimulation index for an individual animal. (C) Multiple combination staining ($CD3^+CD44^+CD62L^+$ $CD25^+$ $CD69^{2+}$ $CD4^+$ or $CD8^+$) was also employed to identify central memory T lymphocytes, and cell proliferation following re-stimulation with recombinant NP is shown as mean stimulation indices (n = 5). Statistical significance of differences between groups was considered by one-way ANOVA and Tukey's multiple comparisons *post hoc* test (**$p < 0.01$)

approaches to vaccine design for rapid response in the face of viral outbreaks.[31] In this context, synthetic biological approaches offer a number of powerful advantages. The present work describes such a synthetic approach, combining the strengths of RepRNA complexed with lipid-based formulations.[1,3]

RNA offers advantages over DNA by removing the requirement for nuclear translocation, which is negligible in non-proliferating cells,[32] and even T7 promoter DNA plasmids have shown only limited clinical application.[33] Self-amplifying RNA, as with the RepRNA potential to self-replicate, provides additional advantages over mRNA for vaccine purposes; the replicative nature increases the duration of antigen presence for stimulating robust immune defenses and the potential for promoting both humoral and cell-mediated immune defenses.[1] Although Alphavirus replicons packaged within VRPs have vaccine potential,[1,8,11,13,34,35] such replicons are cytopathogenic, thus encumbering the biological role of DCs in promoting immune defenses.[1] Employing non-cytopathogenic RepRNA, such as those derived from CSFV genomes, offers the advantage of prolonged antigen production within the cell of interest without destruction of the targeted cell; RepRNA constructs derived from CSFV genomes offer further advantages because virulence cannot be acquired in humans.

Conversely, RNA-based vaccines are highly sensitive to enzymatic destruction, and efforts to modify cellular function through transfer of naked nucleic acid has repeatedly proven ineffective.[36,37] This has been countered by RepRNA delivery in the aforementioned packaged VRPs.[1,8,10–13,34] Disadvantages with packaging as VRPs include the requirement for complementing cells supplying the deleted gene of the RepRNA. Moreover, VRPs are antigenic and, therefore, a potential target for the immune system per se as a result of pre-disposed immunity. VRPs may also exhibit tropisms towards cell types other than DCs and are often restricted for application in certain species. As an alternative, supramolecular carriers such as cationic lipids can enhance the efficiency and activity of the nucleic acid by providing both the necessary protection from enzymatic degradation and targeting to the desired cell type.[1,38–43]

Synthetic nanoparticle delivery vehicles, including lipids, chitosans, and polymers, have been applied for delivery of proteins, DNA or small interfering RNA (siRNA) molecules.[1,44] Tratschin et al.[4] were the first to describe the potential of such large RNA molecules as vaccines when delivered using biodegradable nanoparticulate vehicles.[1] This gave rise to successful delivery of RepRNA vaccines to DCs *in vitro* and *in vivo* using chitosan-based vehicles, particularly when combined with cationic lipids.[1] This work has been elaborated to include successful polyethyleminine-polyplex-based delivery of RepRNA to DCs.[2] Clearly, the application of chitosan-based nanoparticles benefited from the additional presence of cationic lipids. Accordingly, the present work sought to determine whether cationic lipids in their own right would prove to be efficient at delivering such large RNA molecules to DCs for translation.

Although cationic lipids have been applied with a large variety of nucleic acids, they have never been demonstrated to facilitate the specific transfection of large RepRNA (>14 kb) into DCs. With DCs being an important target because of their critical roles in controlling and promoting immune defense development,[16,17] the present work assessed delivery of the relatively large RepRNA molecules for translation in DCs.

The general structure of cationic lipids comprises a hydrophobic symmetric or di-symmetric, saturated or unsaturated, modified or unmodified, linear or branched chain attached to a cationic head group with a linker molecule that can be cleavable to favor biodegradation or not. The head group usually contains at least one group, such as

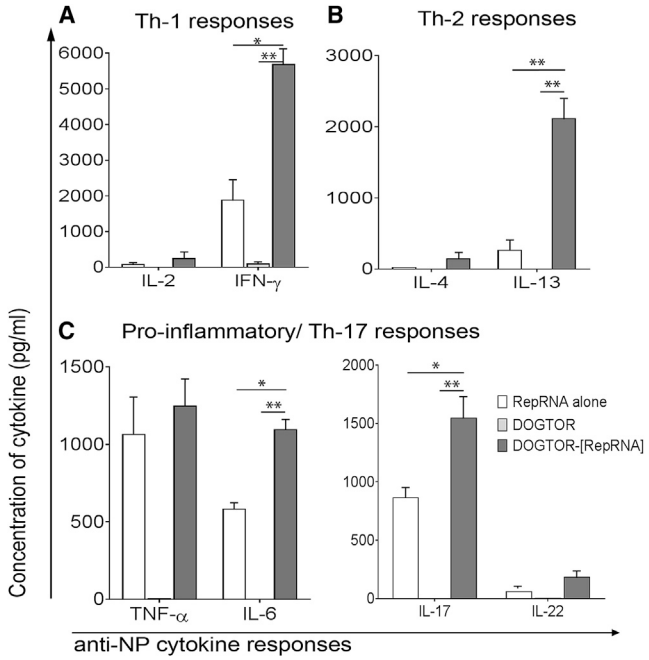

Figure 7. Cytokine Analysis from Sera Collected from Vaccinated Animals as Assessed with Cytometric Bead Arrays

(A–C) Experimental animals (n = 5) received a subcutaneous vaccination cocktail of 0.4 μg of NP-RepRNA complexed with DOGTOR. The vaccination cocktail was adjuvanted with PEGylated MALP-2. RepRNA alone and DOGTOR alone were used as control groups. Splenocytes were processed and cultured and received 1 μg/mL of recombinant NP. Supernatants were collected 96 hr after re-stimulation of splenocytes (day 84 post-vaccination) and assessed for cytokine content. Results are shown as (A) Th-1, (B) Th-2, and (C) pro-inflammatory Th-17-associated cytokine responses. Statistical significance of differences between groups was considered by one-way ANOVA and Tukey's multiple comparisons post-hoc test (*$p < 0.05$, **$p < 0.01$).

amine, that acquires a positive charge at physiological pH levels.[45] Therefore, cationic lipids can be complexed with cargoes, allowing the appropriate electrostatic interactions to occur.[46] With lipoplexes, their characteristics are governed by the lipid composition and nature, including the helper lipid, providing the strength of electrostatic charges between the lipid and nucleic acid.[47] Importantly, a lipid function cannot be extrapolated on the basis of lipid structure alone, and no real structure-function relationship has been demonstrated. The variety of parameters involved renders this structure-function relationship study extremely difficult. Characteristics that could provide clues regarding function include the overall size, ζ-potential homogeneity, shape of the lipoplexes, ability to bind to cell surfaces, and capacity to deliver and release their cargo intracellularly. Accordingly, the present study assessed lipids with different numbers of amine groups; Lullaby carries the least number of cationic charges whereas NL-10 carries the most. These different lipids efficiently delivered RepRNA to DCs. The lipids were clearly classified into two groups: NL-10, NL-21, and NL-42 carriers were more efficient for intracellular delivery. DOGTOR, Dreamfect, and Lullaby were less efficient but still capable of delivering RepRNA to DCs and also showed minimal cytotoxicity. Although amine groups should result in stronger interactions between lipid and RepRNA molecules, potentially forming lipoplexes with greater stability, this could explain the differential efficiency of associating with DCs. Thermodynamic interactions between the negatively charged nucleic acid and the cationic lipid amine groups[46] promotes charge strengths affecting the final geometry of the lipoplex structure and, possibly, transfection efficiency. Eventually, the lipids should wrap around the nucleic acid molecules, forming a "stable: compact structure.[48,49] Differences in cationic charges and hydrophobicity between different lipids would result in varying patterns of packing constraints during lipoplex formation and, therefore, affect the complex geometry.

The presence of DOPE lipid molecules is considered vital for balancing the cationic charges and facilitating intracellular release by endosomal membrane destabilization and may facilitate looser interactions between the cationic lipids and nucleic acids. Cationic lipids adopt various structural phases in an aqueous environment,[50] which can influence intracellular membrane stability and cytosolic translocation of nucleic acids.[51] The size measurements of the different lipoplexes demonstrated efficient compaction of RepRNA molecules (parcels of approximately 150 nm), with NL-10, NL-21, and NL-42-based lipoplexes appearing slightly smaller than other lipoplexes. In contrast, Lullaby lipoplexes were particularly large with a lower ζ-potential, suggesting considerably looser complexing in larger nanoparticles. Nonetheless, translation of RepRNA molecules could only be detected with lipoplexes showing lower delivery efficiencies, particularly DOGTOR. When comparing two lipids of the aforementioned different classes, DOGTOR and NL-10, confocal microscopy demonstrated that the interaction with DCs was mostly cell surface binding, despite NL-10 having more amine groups in its head group. It is therefore considered that the final geometry of the lipoplexes may determine whether internalization by DCs will be favored beyond binding at the cell surface.

The delivery of protected RepRNA molecules is only the initial stage for successful synthetic nanoparticulate RepRNA vaccines. Translocation to cytosolic compartments together with adequate decompaction is essential for the RepRNA to access cellular translation sites. The results provided evidence that cationic lipid vehicles can indeed deliver large complex RepRNA molecules for translation in DCs. Again, it was the lipids showing less efficiency for delivery that more successfully facilitated RepRNA translation, particularly DOGTOR or Dreamfect lipoplexes. Interestingly, both lipids have the same number of amine groups. The results also demonstrated, with Dreamfect-RepRNA complexes, that RNA translation could be detected in the absence of notable levels of delivery when assessed with confocal microscopy.

It was considered that the differences observed in lipoplex delivery and translation with the different lipids may be sensitive to the RepRNA cargo concentration employed, as reported for chitosan nanoparticle delivery of RepRNA.[1,3] When DOGTOR- and NL-10-based lipoplexes carrying increasing loads of RepRNA molecules

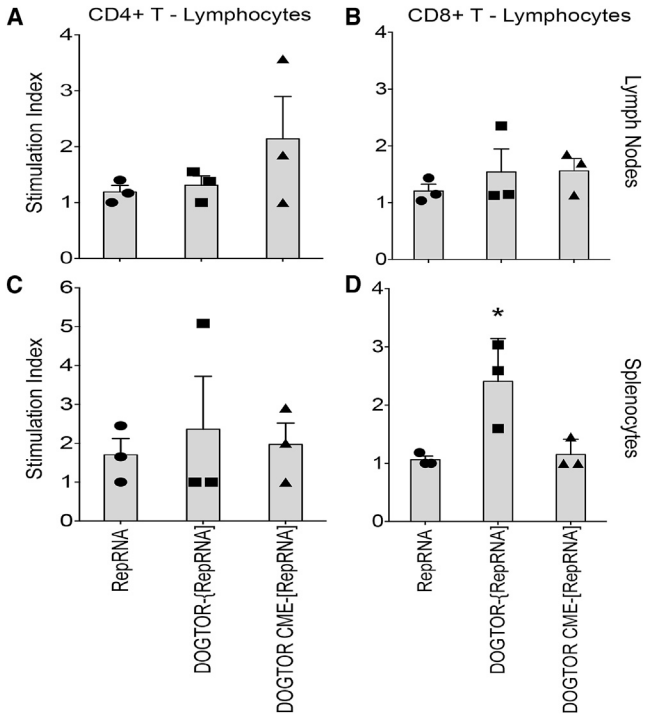

Figure 8. Lipoplexes Evoke Antigen-Specific Responses in Transgenic TCR Mice that Recognize Residues of the Ovalbumin Protein

The RepRNA constructs received the ovalbumin-encoding gene cassette at the 3′ end of the C gene and the N^{pro} gene. The constructs also received an encephalomyocarditis (EMCV) internal ribosomal entry site (IRES) cassette to ensure continuous smooth translation of the RepRNA. BMDCs from OVA-transgenic animals were pulsed with DOGTOR-RepOVA complexes, and 3 days later, recipient animals received treated BMDCs. Cell proliferation was quantified in lymph nodes (A and B) and splenocytes (C and D) of recipient animals as a reduction of CFSE signal as percent of central memory $CD4^+$ (A and C) and $CD8^+$ (B and D) T cells gated as $CFSE^{low}$, indicating cell division. Stimulation indices were determined relative to the percent of cells gated as $CFSE^{low}$ obtained in the non-stimulated control. Data are shown as mean stimulation indices, with each dot representing the stimulation index for an individual animal (n = 3). Statistical significance of differences between groups was considered by one-way ANOVA and Tukey's multiple comparisons *post hoc* test (*$p < 0.05$).

were assessed for delivery and translation *in vitro*, a problem with the higher concentrations of NL-10 was noted whereby large aggregates of lipoplexes were observed. Clearly, this would affect the mode of cellular uptake and subsequent processing by the cell. Nonetheless, there was no clear effect on either the size or charge of the complexes. This simple approach of increasing the RepRNA delivery load did increase the detectability of internalized molecules. Indeed, detection of translation following NL-10-assisted delivery of RepRNA was now possible. It is likely that increasing the RepRNA influenced the final geometry of the lipoplex. However, there remained the problem associated with the apparent increase in aggregation, which could prove problematic for the targeted cells, particularly *in vivo*. Alternatively, aggregates may offer an advantage when related to the observations on vaccine adjuvants, providing what is referred to as the depot effect.[52]

Considering the successful *in vitro* translation data with lower RepRNA cargoes and the absence of detectable cytotoxicity or aggregation together with its consistency in transfection, DOGTOR was selected for *in vivo* assessment. DOGTOR-mediated delivery of RepRNA molecules did provide for translation *in vivo*, as witnessed by the induction of antibody (B lymphocyte responses require translation of intact antigen molecules) and processing of translated antigen into peptides for inducing immunological help. This observed humoral response was reinforced by the proliferative capacity of memory B lymphocytes. T lymphocyte cellular proliferative responses were also enhanced in mice receiving DOGTOR-RepRNA complexes. The specific cytokine responses induced—including IFN-γ, IL-4, IL-6, and IL-22—suggest a balanced Th1/Th2/Th17 response. IFN-γ and IL-4 would be important for antibody class switch,[53] whereas IL-17 would be involved in DC maturation and T cell differentiation as well as recruitment of effector and naive T cells.[54,55] IL-22 would play an important role in immunoregulatory mechanisms when establishing vaccine-induced memory responses.[56] In accordance with previous observations,[2,3] naked RepRNA was unable to evoke any antibody or cellular proliferative responses.

It is important to note that the above results were obtained by co-formulating the lipoplexes with the adjuvant MALP-2 in the vaccine cocktail, which offers a formulation providing clarity regarding the benefits of lipid-based nanoparticle RepRNA delivery systems. For *in vivo* efficacy, it is considered that the presence of such an efficacious adjuvant should be of major significance. Accordingly, we are currently investigating whether the adjuvant should be part of the lipoplex architecture itself or whether it would be more beneficial when co-administered in the vaccine cocktail. Studies will also elaborate on the lipoplex formulation to determine how different methods of formulation influence the characteristics of lipid-mediated RepRNA delivery.

It is also recognized that active immunosurveillance by specific rapidly proliferating T cells is an essential component of a robust immune defense. Accordingly, we assessed DOGTOR-assisted RepRNA delivery with a T cell receptor (TCR)-transgenic OT-I and OT-II model using an OVA-RepRNA construct. Activation of both $CD4^+$ and $CD8^+$ T cell proliferation was observed with splenocytes from the vaccinated animals. This suggested that lipoplex formation between appropriately selected cationic lipids and RepRNA is central for successful formulation leading to translation of delivered RepRNA.

Our present work characterizes, for the first time, self-replicating RepRNA interaction with cationic lipids for delivery to DCs. To our knowledge, there are no reports using cationic lipids for the delivery of such non-cytopathic RepRNA molecules, with previous work focusing on small RNA and DNA molecules. It is generally accepted that cationic lipids should deliver their cargo through endocytic pathways; therefore, we focused on assessing the relative efficiency of different lipoplexes to interact with DCs. RepRNA can only be of value when delivered unharmed to the cytosolic compartment of cells. Gaining important insight into lipoplex trafficking in DCs, in particular leading to RepRNA translation, is important for defining efficient

transfection to ultimately promote immune response development. Accordingly, we have identified the form of cationic lipid molecule providing the most efficient lipoplexing that facilitates delivery leading to translation of RepRNA in DCs both *in vitro* and *in vivo*. An important aspect is that efficiency of delivery does not guarantee efficiency of translation, probably related to the degree of RepRNA compaction in the lipoplexes. Creating the appropriate balance between compaction to protect and deliver the RepRNA and subsequent decompaction within DCs to facilitate cytosolic translocation for translation of the RepRNA is a determining factor in the successful development of lipoplex vaccines. We also observed that aggregation can prove to be detrimental, whereas appropriate formulation with efficacious adjuvants such as MALP-2 is paramount for success *in vivo*.

MATERIALS AND METHODS

RepRNA Plasmid Constructs

Generation of the RepRNA constructs employed in the present work was as described by Démoulins et al.[57] The pA187-1 plasmid was used for these investigations; it carries the full-length cDNA clone of the non-cytopathogenic CSFV strain Alfort/187 (GenBank: X87939).[58] The viral structural gene E^{rns} was removed from the cDNA sequence; however, the RepRNA houses the *NotI* endonuclease restriction site employed to introduce or exchange new genes of interest. A more detailed description of the construction of these self-replicating RNA constructs as well as generating VRP-packaged RepRNA can be found in McCullough et al.[3] and Démoulins et al.[57] The Label IT Fluorescein Nucleic Acid Labeling Kit was used to label RepRNA at 1:1 reagent/RepRNA weight ratio.

Experimental Animals

The experiments with 6- to 8-week-old female BALB/c mice (obtained from Charles River Laboratories, France) were performed at the animal facility of the Institute of Virology and Immunology in Mittelhäusern, Switzerland in compliance with the Swiss Animal Welfare Act and the related ordinances. All studies were reviewed by the ethical committee for animal experiments of the canton of Bern and approved by the cantonal veterinary authorities (Amt für Landwirtschaft und Natur LANAT, Veterinärdienst VeD, Bern, Switzerland) with license BE72/12. The mice were provided with environmental stimuli (bedding and nesting material); food pellets (KLIBA NAFAG, Switzerland) and water were available *ad libitum*, and environmental conditions comprised a 12-hr dark/light cycle at 21°C ± 1°C. Experiments with OVA-TCR transgenic mice, C57BL/6-Tg (TCRαTCRβ) 1100Mjb/J (OT-I) and C57BL/6-Tg (TCRαTCRβ) 425Cbn (OT-II), were conducted at the animal facility of the Helmholtz Centre for Infection Research (Germany) under specific pathogen-free conditions adhering to regulations and in agreement with the ethical committee of the local government of Lower Saxony (German authorities). All experiments were blinded, and the groups were randomized.

Cell Lines

Swine kidney SK-6 cells were provided by Prof. Maurice Pensaert (University of Gent, Belgium). The cells were cultured in modified Eagle's medium (MEM) supplemented with 7% horse serum.

Generation of Porcine DCs

Porcine DCs were the primary cells of choice because of their close association with human DCs as well as their availability in large numbers from a single animal. Density centrifugation on Ficoll-Paque PLUS (GE Healthcare, Glattbrugg, Switzerland) was employed to isolate PBMCs from specific pathogen-free (SPF) pigs bred at the Institute of Virology and Immunology IVI (licenses BE26/11 and BE88/14 from the veterinary authorities of the canton of Bern, Switzerland). Cells were stained with an anti-CD172a monoclonal antibody (mAb) (74-22-15/a, kindly donated by Dr. J. K. Lunney, Department of Agriculture, Beltsville, MD) and $CD172^{low}$ (cDCs and porcine DCs [pDCs]), and $CD172^{hi}$ monocytes were isolated with a magnetic-activated cell sorting system (Miltenyi Biotec). Cells were cultured at 1×10^6 in DMEM supplemented with 10% (v/v) porcine serum (PS) and incubated at 39°C (physiological internal porcine temperature) for the duration of the experiment. Monocyte-derived (Mo)-DCs were also generated by culturing CD172a-selected cells in the presence of 50 U/mL porcine granulocyte-macrophage colony-stimulating factor (GM-CSF) and 100 U/mL IL-4 for 5 days at 39°C.

Characterization of Lipid-(RepRNA) and Lipid-(oliRNA) Complexes

Lipoplexes were generated using the different lipidic formulations (kindly provided by OZ Biosciences, Marseille, France) with different concentrations of RepRNA but maintaining a ratio of 3:1 (lipid:nucleic acid), by admixing for 20 min at room temperature, as described by Démoulins et al.[57] Biodegradable amino acid-based cationic liposomes were synthesized (OZ Biosciences) in RNase-free water in the absence or presence of different volumes of the neutral DOPE helper lipid, with final cationic charges ranging between 2–6. For lipoplexes, 5 μg of replicon was diluted into 250 μL aqueous solution of sodium chloride ($Na^{2+}Cl^{-}$, 145 mM). 20 μg of each lipid was diluted into 100 μL $Na^{2+}Cl^{-}$ 145 mM. Complexes were prepared by mixing 25 μL (1 μg) of replicon with 25 μL (3 μL lipid) lipid aqueous solution and allowed to stand for 20 min at room temperature. Prepared complexes were treated with 10 μL dextran sulfate solution (0.5–4 mg/mL, Sigma-Aldrich) or TRIzol (>95%, Ambion) for 20 min at room temperature to assess the capacity of the different lipids to associate with RepRNA. With regard to TRIzol treatment, the complexes were treated with 1 mL of TRIzol 20 min after the lipids were allowed to complex the replicon, and subsequently chloroform was added for phase separation. RNA was precipitated using isopropyl alcohol, and after 2 cycles of ethanol washing, the pellet was re-suspended in RNase-free water. RNA dissociation from complexes or the lack thereof was assessed with electrophoresis on a 1% agarose gel for 10–15 min at 130 V.

Assessment of the lipoplexes determined characteristics that were pertinent to understanding how the delivery formulations might influence interaction with DCs, this area being the main focus of this study. These characteristics were as follows: size, described as a crucial factor for nanomaterial characterization;[59] surface properties that respond to the interactions of the nanomaterial with surrounding species;[60] shape and encapsulation capacity, known to play an important role in drug delivery, degradation, transport, targeting, and internalization;[61] and

ζ-potential, giving both electrical potential and indications of potential stability and/or aggregation. The mean hydrodynamic diameters and ζ-potentials of the lipids and lipid-(RepRNA) lipoplexes were determined by photon correlation spectroscopy using a Zetasizer Nano Series ZEN3600 (Malvern Instruments). Samples were diluted into 1 mL of PBS solution and transferred into a disposable plastic cuvette for measurement, and data were acquired at 25°C using 173° backscatter detection. ζ-potentials were derived from the electrophoretic mobility using the Helmholtz-Smoluchowski equation.

Flow Cytometric Analysis of Lipoplex-Mediated RepRNA Uptake and Translation

CD172a-selected PBMCs or Mo-DCs were cultured at 1×10^6 in the presence of 10% PS overnight in 24-well or 12-well plates (Nunc, Wiesbaden, Germany) in phenol red-free DMEM. Cells were pulsed with cationic lipids alone, complexed with fluorescein-labeled RepRNA, or RNA alone for 2 hr at 39°C. VRPs were employed as a control. At the end of the incubation period, the cells were assessed for RepRNA delivery or the medium was replaced with fresh, pre-warmed 10% PS-enriched DMEM, and the RepRNA was allowed to translate for 48, 72, or 96 hr at 39°C. Cell preparations were prepared in parallel to assess both RepRNA delivery and translation, and the cells received the same lipid-RepRNA complexes at the same time.

To assess RepRNA delivery to DCs and monocytes, at the end of the incubation period (2 hr) with the various lipoplex formulations, the cells were washed with cold PBS/EDTA and incubated with primary antibodies directed against CD172a (74-22-15/a), CD14 (MIL-2, CAM36A), MHC class II (TH16B), and CD80/86 (CD152-mu immunoglobulin [Ig]) for 20 min on ice. Cells were washed and subsequently incubated with secondary antibodies (BV421, phycoerytrhin [BD Biosciences, Switzerland]; PE-Cy7 [Abcam, Switzerland]; Alexa 647 [Molecular Probes, Leiden Netherlands]).

To assess RepRNA translation cells were incubated with the respective primary antibodies (CD172a-FITC, CD14-PE, and CD86) and subsequently fixed with 4% (w/v) paraformaldehyde (PFA, Sigma-Aldrich) for 10 min at room temperature. Cells were then stained with antibodies directed against anti-NS3 (C16) and anti-NP (HB65), diluted in 0.3% (w/v) saponin (Serwa, Sigma-Aldrich), for 20 min on ice. Following a wash with 0.1% (w/v) saponin, the cells were incubated with secondary conjugated antibodies (BV421 [BD Biosciences, Switzerland]; Alexa 647 [Molecular Probes, Leiden Netherlands]; PE-Cy7 [Abcam, Switzerland]) for 20 min on ice. Following a last wash, cells were re-suspended in sodium azide buffer (0.05%, v/v), and cell acquisition was performed with either a FACS Calibur analytical flow cytometry (FCM) or a FACS Canto analytical FCM (Becton Dickinson, Basel, Switzerland) and analysis employed both FlowJo versions 9 and 10 (Tree Star, San Carlos, CA).

Analysis of Lipoplex-Mediated RepRNA Translation Using Confocal Microscopy

Primary porcine CD172a-enriched PBMCs or Mo-DCs were cultured at 200,000 in 8-well Lab-Tek II (Nunc) chambers pre-coated with fibronectin. The cells were incubated in phenol red-free DMEM enriched with 10% (v/v) PS, and cells were pulsed with the various RepRNA lipoplexes for 2 hr at 39°C. At the end of incubation, the medium was replaced with fresh pre-warmed conditioned medium (DMEM enriched with 10% [v/v] PS, 50 U/mL porcine GM-CSF and 100 U/mL IL-4). The cells were allowed 72 hr at 39°C before being assessed for RepRNA translation using the procedure described above. Following incubation with secondary conjugated antibodies, the cells were washed with PBS, and the slides were mounted in Mowiol. Images were acquired using a 63× objectives mounted on a Leica TCS-SL confocal microscope (Leica Microsystems, Glattbrugg). The settings and voxel size were adjusted to acquire high-resolution images. Image analysis was performed with IMARIS software versions 7.5 and 7.6 (Bitplane, Zurich, Switzerland).

Assessing Responses of Lipoplex-Mediated Delivery of RepRNA *In Vivo*

RepRNA was complexed with the lipid of choice, and 100 μL were used per dose of vaccination of BALB/c mice. The vaccination cocktail was prepared with 0.4 μg in 50 μL NP-RepRNA for each dose per mouse. The cocktail was supplemented with 10 μg of PEGylated MALP-2 adjuvant as described previously.[62] Each animal received a subcutaneous vaccination (on days 0, 28, and 56) on the ventral aspect and was bled from the saphenous vein on a bi-weekly basis. Anti-NP IgG antibody titers were quantified using an indirect ELISA and recombinant NP (H_3N_2, Brisbane 2007) as antigen.

Splenocytes as well as inguinal and axillary lymph nodes were collected following termination of the animals, 4–5 weeks after the last booster vaccination. Both lymphoid organs were washed and separately disrupted through a plastic mesh. Splenocytes were treated with 0.83% (w/v) NH_4Cl treatment to lyse the erythrocyte populations, whereas the lymph nodes were treated with 1 mg/mL collagenase-D (Roche, Switzerland) and 0.1 mg/mL DNase (Roche, Switzerland) prepared in 0.035% (w/v) EDTA-PBS (Ca^{2+}/Mg^{2+}-free) to lyse the lymph node fibrous capsule. Single-cell suspensions were labeled with carboxy fluorescein succinimidyl ester (CFSE) (5 μM, BioLegend, Fell, Germany) to assess cell division and were thoroughly washed with 0.035% (w/v) EDTA-PBS (Ca^{2+}/Mg^{2+}-free) before re-suspended in RPMI 1640 medium enriched with 10% (v/v) FCS. Both splenocytes and lymph node cells were cultured at either 3×10^6 /mL and were left non-stimulated (no antigen) or received 1 μg/mL hemagglutinin (HA) or NP. On day 5, the presence of the stimulant was replenished with fresh pre-warmed supplemented medium. On day 7, the cells were harvested and stained with multicolor combination staining that allowed gating on central memory T lymphocytes or memory B cells.

For B lymphocyte analysis, cells were stained with CD19 (6D5), CD45R (RA3-6B2), IgD (11-26c.2a), IgM (RMM-1), CD24 (SN3) (BioLegend, Fell, Germany), and CD21 (BD Biosciences, Switzerland). Memory B cells were identified as $CD19^+$, $CD45R^+$, IgD^{low}, IgM^{low}, $CD24^+$, and $CD21^+$. Proliferating "daughter" B lymphocytes were identified by reduced CFSE expression ($CFSE^{low}$).

A stimulation index was calculated relative to the percent positives obtained for the unstimulated population ($CFSE^{low}$). For T lymphocyte analysis, cells were stained for CD3 (17A2), CD4 (GK1.5), CD8a (53-6.7), CD44 (IM7), CD62L (MEL-14), and CD69 (H1.2F3) (BioLegend, Fell, Germany) expression with primary directly conjugated antibodies. Central circulating effector memory T lymphocytes were identified as $CD4^+$ or $CD8^+$ $CD3^+$, $CD44^{hi}$, $CD62L^{hi}$. Cell proliferation was assessed as described for B lymphocytes; however, CD69 upregulation was also used as an indicator of central memory T lymphocyte proliferation. Cell acquisition was performed with a FACS Canto analytical FCM (Becton Dickinson, Basel, Switzerland) with 8×10^5 events recorded, and analysis employed both FlowJo versions 9 and 10 (Tree Star, San Carlos, CA).

Assessment of OVA-Specific Responses

Bone marrow-derived DCs (BMDCs) were cultured from OT-I and OT-II donor mice using already established protocols before being pulsed with naked RepRNA or RepRNA-OVA-DOGTOR for 2 hr. Lipid-RepRNA complexes were prepared with 2 μg of OVA-RepRNA adhering to pre-established protocols. Cells were washed to remove excess non-internalized lipid complexes, and the RepRNA was allowed to translate for the following 72 hr before the BMDCs were injected into recipient OT-I or OT-II mice, respectively. Each animal received a subcutaneous vaccination on the ventral aspect. The animals were euthanized 7 days later, and the spleen and lymph nodes were collected to assess OVA-specific responses.

Cytokine Profiles

The secretion of serum cytokines and chemokines from antigen-specific immune cells following re-stimulation with either recombinant NP at 1 μg/mL (at 37°C for 96 hr) was assessed using the mouse Th1/Th2 FlowCytomix cytokine array (IL-2, IL-4, IL-5, IL-6, IL-13, IL-17, TNF-α, and IFN-γ), adhering to the manufacturer's instructions (eBioscience, Bender MedSystems, USA; BioLegend 13plex mouse Th cytokine panel) and as described previously.[62]

Statistical Analyses

Numerical data were analyzed using GraphPad Prism 6.0/7.0, and multiple comparisons were considered using one-way ANOVA. Dunnett's multiple comparisons *post hoc* test was employed for comparisons with a control group, and Tukey's test was employed when comparisons were made between all treatment groups. Significant differences are illustrated as follows: $^{***}p < 0.001$, $^{**}p < 0.01$, and $^{*}p < 0.05$.

SUPPLEMENTAL INFORMATION

Supplemental Information includes Supplemental Materials and Methods, three figures, and one table and can be found with this article online at https://doi.org/10.1016/j.omtn.2018.04.019.

AUTHOR CONTRIBUTIONS

All authors contributed important elements to the work presented herein. P.C.E. designed and performed the various experiments, assembled the data, prepared the figures, and wrote the manuscript. P.C.E. designed and generated the Rep-OVA construct. N.R. generated the base replicon constructs from which all others were derived, designed the new constructs with the second linearization site, trained P.C.E. and T.D., and supervised all replicon production. P.C.E. and T.D. generated all other RepRNA constructs and produced all RNA for all experiments. C.S. together with F.P. synthesized, characterized, and performed quality control assessments on the OZ Biosciences lipids employed for both the *in vitro* and *in vivo* studies under the supervision of O.Z. C.S. and F.P. contributed to the characterization of the lipoplexes under the overview and direction of O.Z. P.C.E., T.D., P.M., and N.R. contributed to the design and execution of the *in vivo* mouse experiments using the NP-replicon, to the analysis of the results, and to the production and quality control assessment of the RepRNA employed. T.E., K.S., and C.-A.G. contributed to the design and execution of the mouse *in vivo* experiments using the OVA replicon. T.D. contributed to the design and implementation of supplemental *in vitro* experiments and their analysis and to the analysis of the *in vivo* experimental samples. P.M. performed the anti-NP ELISA. T.E. and K.S. performed all immunological analyses on the OVA-replicon-vaccinated mice and all cytokine analyses. K.C.M. oversaw the design of the various experiments and edited the manuscript with input from C.-A.G., T.E., and O.Z. All authors discussed the results and commented on the manuscript.

CONFLICTS OF INTEREST

Patents for the application of delivery vehicles for the delivery of RepRNA vaccines to DCs[3] using replicons derived from classical swine fever virus, as employed in this paper, have been filed in Europe, USA, Canada, and Japan with a priority date of 2008. The filing was done by K.M. and N.R. together with Jon Duri Tratschin (all three as inventors) (WO 2009146867)[4] and assigned to their employer, the Institute of Virology and Immunology. C.-A.G. and T.E. are named as inventors in patents covering the use of c-di-AMP as adjuvant (PCT/EP 2006010693, EP/04.04.02/EPA 02007640, and PCT/EP2006011182). This does not alter the authors' adherence to the policies of sharing data and materials.

ACKNOWLEDGMENTS

These investigations were supported by Swiss National Science Foundation Project RNA-Targeting (310030-150008), EU FP7 Project UNIVAX (HEALTH-F3-2013-60173), and Marie-Curie Action FP7-PEOPLE-2009-IAAP "Replixcel" (251420). We give special thanks to Brigitte Hermann for help with the culture of cell lines as well as for help with the preparation of RepRNA molecules from the plasmid DNA constructs. Gratitude is also due to Andreas Michel and Hans-Peter Lüthi for ensuring correct animal care and for collecting blood for PBMC isolation.

REFERENCES

1. McCullough, K.C., Bassi, I., Démoulins, T., Thomann-Harwood, L.J., and Ruggli, N. (2012). Functional RNA delivery targeted to dendritic cells by synthetic nanoparticles. Ther. Deliv. 3, 1077–1099.

2. Démoulins, T., Milona, P., Englezou, P.C., Ebensen, T., Schulze, K., Suter, R., Pichon, C., Midoux, P., Guzmán, C.A., Ruggli, N., and McCullough, K.C. (2016).

Polyethylenimine-based polyplex delivery of self-replicating RNA vaccines. Nanomedicine (Lond.) *12*, 711–722.

3. McCullough, K.C., Bassi, I., Milona, P., Suter, R., Thomann-Harwood, L., Englezou, P., Démoulins, T., and Ruggli, N. (2014). Self-replicating Replicon-RNA Delivery to Dendritic Cells by Chitosan-nanoparticles for Translation In Vitro and In Vivo. Mol. Ther. Nucleic Acids *3*, e173.
4. Tratschin, J.D., Ruggli, N., and McCullough, K.C. (2008). Pestivirus replicons providing an RNA-based viral vector system. US patent application publication 20160108372 A1, filed December 22, 2015, and published April 21, 2016.
5. Brito, L.A., Chan, M., Shaw, C.A., Hekele, A., Carsillo, T., Schaefer, M., Archer, J., Seubert, A., Otten, G.R., Beard, C.W., et al. (2014). A cationic nanoemulsion for the delivery of next-generation RNA vaccines. Mol. Ther. *22*, 2118–2129.
6. Geall, A.J., Verma, A., Otten, G.R., Shaw, C.A., Hekele, A., Banerjee, K., Cu, Y., Beard, C.W., Brito, L.A., Krucker, T., et al. (2012). Nonviral delivery of self-amplifying RNA vaccines. Proc. Natl. Acad. Sci. USA *109*, 14604–14609.
7. Brazzoli, M., Magini, D., Bonci, A., Buccato, S., Giovani, C., Kratzer, R., Zurli, V., Mangiavacchi, S., Casini, D., Brito, L.M., et al. (2015). Induction of Broad-Based Immunity and Protective Efficacy by Self-amplifying mRNA Vaccines Encoding Influenza Virus Hemagglutinin. J. Virol. *90*, 332–344.
8. Atkins, G.J., Fleeton, M.N., and Sheahan, B.J. (2008). Therapeutic and prophylactic applications of alphavirus vectors. Expert Rev. Mol. Med. *10*, e33.
9. Khromykh, A.A. (2000). Replicon-based vectors of positive strand RNA viruses. Curr. Opin. Mol. Ther. *2*, 555–569.
10. Pijlman, G.P., Suhrbier, A., and Khromykh, A.A. (2006). Kunjin virus replicons: an RNA-based, non-cytopathic viral vector system for protein production, vaccine and gene therapy applications. Expert Opin. Biol. Ther. *6*, 135–145.
11. Rayner, J.O., Dryga, S.A., and Kamrud, K.I. (2002). Alphavirus vectors and vaccination. Rev. Med. Virol. *12*, 279–296.
12. Suter, R., Summerfield, A., Thomann-Harwood, L.J., McCullough, K.C., Tratschin, J.D., and Ruggli, N. (2011). Immunogenic and replicative properties of classical swine fever virus replicon particles modified to induce IFN-α/β and carry foreign genes. Vaccine *29*, 1491–1503.
13. Ljungberg, K., and Liljeström, P. (2015). Self-replicating alphavirus RNA vaccines. Expert Rev. Vaccines *14*, 177–194.
14. McCullough, K.C., Milona, P., Démoulins, T., Englezou, P., and Ruggli, N. (2015). Dendritic Cell Targets for Self-Replicating RNA Vaccines. J. Blood Lymph *5*, 132.
15. McCullough, K.C., Milona, P., Thomann-Harwood, L., Démoulins, T., Englezou, P., Suter, R., and Ruggli, N. (2014). Self-amplifying replicon RNA vaccine delivery to dendritic cells by synthetic nanoparticles. Vaccines (Basel) *2*, 735–754.
16. Mellman, I., and Steinman, R.M. (2001). Dendritic cells: specialized and regulated antigen processing machines. Cell *106*, 255–258.
17. Steinman, R.M., and Pope, M. (2002). Exploiting dendritic cells to improve vaccine efficacy. J. Clin. Invest. *109*, 1519–1526.
18. Kumari, S., Mg, S., and Mayor, S. (2010). Endocytosis unplugged: multiple ways to enter the cell. Cell Res. *20*, 256–275.
19. Platta, H.W., and Stenmark, H. (2011). Endocytosis and signaling. Curr. Opin. Cell Biol. *23*, 393–403.
20. Luo, D., and Saltzman, W.M. (2000). Synthetic DNA delivery systems. Nat. Biotechnol. *18*, 33–37.
21. Lundstrom, K. (2016). Replicon RNA Viral Vectors as Vaccines. Vaccines (Basel) *4*, E39.
22. Andries, O., Kitada, T., Bodner, K., Sanders, N.N., and Weiss, R. (2015). Synthetic biology devices and circuits for RNA-based 'smart vaccines': a propositional review. Expert Rev. Vaccines *14*, 313–331.
23. Rodríguez-Gascón, A., del Pozo-Rodríguez, A., and Solinís, M.A. (2014). Development of nucleic acid vaccines: use of self-amplifying RNA in lipid nanoparticles. Int. J. Nanomedicine *9*, 1833–1843.
24. Zelphati, O., and Moutard, S. (2009). New class of cationic lipids for transporting active agents into cells. US patent application publication US20120015865 A1, filed February 16, 2011, and published January 19, 2012.
25. Zelphati, O., and Szoka, F.C., Jr. (1996). Mechanism of oligonucleotide release from cationic liposomes. Proc. Natl. Acad. Sci. USA *93*, 11493–11498.
26. Hattori, Y., Hara, E., Shingu, Y., Minamiguchi, D., Nakamura, A., Arai, S., Ohno, H., Kawano, K., Fujii, N., and Yonemochi, E. (2015). siRNA delivery into tumor cells by cationic cholesterol derivative-based nanoparticles and liposomes. Biol. Pharm. Bull. *38*, 30–38.
27. Auray, G., Keller, I., Python, S., Gerber, M., Bruggmann, R., Ruggli, N., and Summerfield, A. (2016). Characterization and Transcriptomic Analysis of Porcine Blood Conventional and Plasmacytoid Dendritic Cells Reveals Striking Species-Specific Differences. J. Immunol. *197*, 4791–4806.
28. Link, C., Gavioli, R., Ebensen, T., Canella, A., Reinhard, E., and Guzmán, C.A. (2004). The Toll-like receptor ligand MALP-2 stimulates dendritic cell maturation and modulates proteasome composition and activity. Eur. J. Immunol. *34*, 899–907.
29. Borsutzky, S., Fiorelli, V., Ebensen, T., Tripiciano, A., Rharbaoui, F., Scoglio, A., Link, C., Nappi, F., Morr, M., Buttó, S., et al. (2003). Efficient mucosal delivery of the HIV-1 Tat protein using the synthetic lipopeptide MALP-2 as adjuvant. Eur. J. Immunol. *33*, 1548–1556.
30. Rharbaoui, F., Drabner, B., Borsutzky, S., Winckler, U., Morr, M., Ensoli, B., Mühlradt, P.F., and Guzmán, C.A. (2002). The Mycoplasma-derived lipopeptide MALP-2 is a potent mucosal adjuvant. Eur. J. Immunol. *32*, 2857–2865.
31. García-Sastre, A., and Mena, I. (2013). Novel vaccine strategies against emerging viruses. Curr. Opin. Virol. *3*, 210–216.
32. Aronsohn, A.I., and Hughes, J.A. (1998). Nuclear localization signal peptides enhance cationic liposome-mediated gene therapy. J. Drug Target. *5*, 163–169.
33. Brisson, M., Tseng, W.C., Almonte, C., Watkins, S., and Huang, L. (1999). Subcellular trafficking of the cytoplasmic expression system. Hum. Gene Ther. *10*, 2601–2613.
34. Lundstrom, K. (2002). Alphavirus-based vaccines. Curr. Opin. Mol. Ther. *4*, 28–34.
35. Zimmer, G. (2010). RNA replicons - a new approach for influenza virus immunoprophylaxis. Viruses *2*, 413–434.
36. Mintzer, M.A., and Simanek, E.E. (2009). Nonviral vectors for gene delivery. Chem. Rev. *109*, 259–302.
37. Tros de Ilarduya, C., Sun, Y., and Düzgüneş, N. (2010). Gene delivery by lipoplexes and polyplexes. Eur. J. Pharm. Sci. *40*, 159–170.
38. Belizaire, R., and Unanue, E.R. (2009). Targeting proteins to distinct subcellular compartments reveals unique requirements for MHC class I and II presentation. Proc. Natl. Acad. Sci. USA *106*, 17463–17468.
39. Granot, Y., and Peer, D. (2017). Delivering the right message: Challenges and opportunities in lipid nanoparticles-mediated modified mRNA therapeutics-An innate immune system standpoint. Semin. Immunol. *34*, 68–77.
40. Riley, M.K., and Vermerris, W. (2017). Recent Advances in Nanomaterials for Gene Delivery-A Review. Nanomaterials (Basel) *7*, E94.
41. Cullis, P.R., and Hope, M.J. (2017). Lipid Nanoparticle Systems for Enabling Gene Therapies. Mol. Ther. *25*, 1467–1475.
42. Jiang, L., Vader, P., and Schiffelers, R.M. (2017). Extracellular vesicles for nucleic acid delivery: progress and prospects for safe RNA-based gene therapy. Gene Ther. *24*, 157–166.
43. Guan, S., and Rosenecker, J. (2017). Nanotechnologies in delivery of mRNA therapeutics using nonviral vector-based delivery systems. Gene Ther. *24*, 133–143.
44. Hughes, G.A. (2005). Nanostructure-mediated drug delivery. Nanomedicine *1*, 22–30.
45. Rao, N.M., and Gopal, V. (2006). Cell biological and biophysical aspects of lipid-mediated gene delivery. Biosci. Rep. *26*, 301–324.
46. Tresset, G. (2009). The multiple faces of self-assembled lipidic systems. PMC Biophys. *2*, 3.
47. Dan, N., and Danino, D. (2014). Structure and kinetics of lipid-nucleic acid complexes. Adv. Colloid Interface Sci. *205*, 230–239.
48. Caracciolo, G., Pozzi, D., Amenitsch, H., and Caminiti, R. (2005). Multicomponent cationic lipid-DNA complex formation: role of lipid mixing. Langmuir *21*, 11582–11587.

49. Oberle, V., Bakowsky, U., Zuhorn, I.S., and Hoekstra, D. (2000). Lipoplex formation under equilibrium conditions reveals a three-step mechanism. Biophys. J. *79*, 1447–1454.

50. Hsu, W.L., Chen, H.L., Liou, W., Lin, H.K., and Liu, W.L. (2005). Mesomorphic complexes of DNA with the mixtures of a cationic surfactant and a neutral lipid. Langmuir *21*, 9426–9431.

51. Wasungu, L., and Hoekstra, D. (2006). Cationic lipids, lipoplexes and intracellular delivery of genes. J. Control. Release *116*, 255–264.

52. Schijns, V.E., and Tangerås, A. (2005). Vaccine adjuvant technology: from theoretical mechanisms to practical approaches. Dev. Biol. (Basel) *121*, 127–134.

53. Nimmerjahn, F., and Ravetch, J.V. (2005). Divergent immunoglobulin g subclass activity through selective Fc receptor binding. Science *310*, 1510–1512.

54. Kawaguchi, M., Adachi, M., Oda, N., Kokubu, F., and Huang, S.K. (2004). IL-17 cytokine family. J. Allergy Clin. Immunol. *114*, 1265–1273, quiz 1274.

55. Kawaguchi, M., Kokubu, F., Odaka, M., Watanabe, S., Suzuki, S., Ieki, K., Matsukura, S., Kurokawa, M., Adachi, M., and Huang, S.K. (2004). Induction of granulocyte-macrophage colony-stimulating factor by a new cytokine, ML-1 (IL-17F), via Raf I-MEK-ERK pathway. J. Allergy Clin. Immunol. *114*, 444–450.

56. Lin, Y., Slight, S.R., and Khader, S.A. (2010). Th17 cytokines and vaccine-induced immunity. Semin. Immunopathol. *32*, 79–90.

57. Démoulins, T., Englezou, P.C., Milona, P., Ruggli, N., Tirelli, N., Pichon, C., Sapet, C., Ebensen, T., Guzmán, C.A., and McCullough, K.C. (2017). Self-replicating RNA vaccine delivery to dendritic cells. Methods Mol. Biol. *1499*, 37–75.

58. Ruggli, N., Tratschin, J.D., Mittelholzer, C., and Hofmann, M.A. (1996). Nucleotide sequence of classical swine fever virus strain Alfort/187 and transcription of infectious RNA from stably cloned full-length cDNA. J. Virol. *70*, 3478–3487.

59. Feng, S.S. (2004). Nanoparticles of biodegradable polymers for new-concept chemotherapy. Expert Rev. Med. Devices *1*, 115–125.

60. Petri, B., Bootz, A., Khalansky, A., Hekmatara, T., Müller, R., Uhl, R., Kreuter, J., and Gelperina, S. (2007). Chemotherapy of brain tumour using doxorubicin bound to surfactant-coated poly(butyl cyanoacrylate) nanoparticles: revisiting the role of surfactants. J. Control. Release *117*, 51–58.

61. Champion, J.A., Katare, Y.K., and Mitragotri, S. (2007). Particle shape: a new design parameter for micro- and nanoscale drug delivery carriers. J. Control. Release *121*, 3–9.

62. Ebensen, T., Libanova, R., Schulze, K., Yevsa, T., Morr, M., and Guzmán, C.A. (2011). Bis-(3′,5′)-cyclic dimeric adenosine monophosphate: strong Th1/Th2/Th17 promoting mucosal adjuvant. Vaccine *29*, 5210–5220.